

The BOLD response and the gamma oscillations respond differently than evoked potentials: an interleaved EEG-fMRI study

Jack R Foucher*¹, H el ene Otzenberger² and Daniel Gounot²

Address: ¹Clinique Psychiatrique – INSERM U405, H opitaux Universitaires – BP 406 – 67091 Strasbourg Cedex – France and ²UMR 7004 – CNRS/ULP – Institut de Physique Biologique, 4 rue Kirschleger – 67085 Strasbourg Cedex – France

Email: Jack R Foucher* - jf@evc.net; H el ene Otzenberger - otzenber@alsace.u-strasbg.fr; Daniel Gounot - gounot@alsace.u-strasbg.fr

* Corresponding author

Published: 19 September 2003

Received: 03 June 2003

BMC Neuroscience 2003, 4:22

Accepted: 19 September 2003

This article is available from: <http://www.biomedcentral.com/1471-2202/4/22>

  2003 Foucher et al; licensee BioMed Central Ltd. This is an Open Access article: verbatim copying and redistribution of this article are permitted in all media for any purpose, provided this notice is preserved along with the article's original URL.

Abstract

Background: The integration of EEG and fMRI is attractive because of their complementary precision regarding time and space. But the relationship between the indirect hemodynamic fMRI signal and the more direct EEG signal is uncertain. Event-related EEG responses can be analyzed in two different ways, reflecting two different kinds of brain activity: evoked, i.e. phase-locked to the stimulus, such as evoked potentials, or induced, i.e. non phase-locked to the stimulus such as event-related oscillations. In order to determine which kind of EEG activity was more closely related with fMRI, EEG and fMRI signals were acquired together, while subjects were presented with two kinds of rare events intermingled with frequent distractors. Target events had to be signaled by pressing a button and Novel events had to be ignored.

Results: Both Targets and Novels triggered a P300, of larger amplitude in the Novel condition. On the opposite, the fMRI BOLD response was stronger in the Target condition. EEG event-related oscillations in the gamma band (32–38 Hz) reacted in a way similar to the BOLD response.

Conclusions: The reasons for such opposite differential reactivity between oscillations / fMRI on the one hand, and evoked potentials on the other, are discussed in the paper. Those results provide further arguments for a closer relationship between fast oscillations and the BOLD signal, than between evoked potentials and the BOLD signal.

Background

There are two core methods to explore human brain function: direct measurement of the electrical activity, as with the electro-encephalogram (EEG), or measurement of the vascular response that is indirectly related to the neuronal activity, as in functional MRI (fMRI) [1]. Because both approaches have complementary advantages, attempts have been made to fuse the high temporal resolution of EEG, with the high spatial resolution of fMRI. Although

animal data have made it possible to elucidate some of the relationships between neuronal activity and the Blood Oxygen Level-Dependant contrast (BOLD) [2–5], there is much left to be worked out about the actual relationship between EEG and fMRI. This paper aims at presenting some data showing, through differential reactivity, that not all kinds of EEG responses might be related to the BOLD contrast.

It has been reported that variations in BOLD contrast in response to the presentation of two kinds of rare events, i.e. oddballs, presented a differential reactivity opposite to that observed using Evoked Potentials (EPs). Oddballs are known to evoke a P300, a positive EP around 300–400 ms [6]. EPs are computed by averaging the EEG signal time-locked to the presentation of a stimulus. Activity time-locked to the stimulus emerges from background EEG activity, which is not time-locked and averages to zero [7]. The P300 is mainly perceived on the medial electrodes (Fz, Cz, Pz), although it originates from the temporo-parietal junction and the inferior frontal gyrus [8–10]. When an oddball has to be detected, i.e. a Target, this potential is of lower amplitude than when it is presented as an event unrelated to the task, i.e. a Novel [6,11,12]. On the other hand, there are fMRI studies in which no Novel-related activation has been reported although the temporal-parietal junction and the inferior frontal gyrus were activated by Targets [13–16].

This study attempts to replicate these findings using combined EEG and fMRI measurements so that both recordings relate to the same brain activity [17,18]. Moreover, Event-Related Oscillations (EROs) were computed in order to reveal brain responses not necessarily time-locked to the stimulus. EROs are computed by averaging the time-frequency decomposition of each peristimulus signal. Accordingly, a small jitter in the initiation of an oscillatory response will not average to zero, which is especially valuable in the high-frequency components [19–21]. EROs in response to auditory oddballs have been described in the gamma band (20–100 Hz), mainly in the 37–40 Hz interval, 360 ms after a Target is presented [22–25]. But the reactivity of EROs to Novels remains to be assessed.

Five subjects were presented with Targets (the letter "X") and Novels (various pictures) mixed with frequent distractors (the letter "O") while EEG and fMRI data were simultaneously recorded. Results are provided as a fixed effect one-tail t-test, and as multi-subject conjunction analysis to ascertain that all the subjects did present the same differential reactivity. The present study replicates the differential reactivity of EPs and BOLD contrast, with respect to Targets and Novels: the P300 was of significantly greater amplitude in response to Novels as opposed to Targets. Oppositely, Targets elicited much more fMRI activation than Novels. In accordance with fMRI results, Target-related gamma oscillations were more intense than their Novel-related counterparts, around 300 ms. The reasons for such opposite differential reactivity between oscillations / fMRI on the one hand, and evoked potentials on the other, are discussed below. Our results support evidence demonstrating that the BOLD signal is

better correlated with high-than with low-frequency oscillations.

Results

Behavioral results

the subjects performed the task with an accuracy rate of $98 \pm 2\%$, with a response time of $474 \text{ ms} \pm 71 \text{ ms}$.

fMRI results

The Target condition is related with activations especially in regions said to be the sources of the P300: the inferior frontal gyrus bilaterally and the right temporo-parietal junction (posterior supramarginal gyrus). Other regions were also activated: the right antero-basal frontal region (BA 10), the anterior cingulate and the supplementary motor areas, bilaterally, the inferior parietal lobule and intraparietal sulcus, and the left central sulcus and thalamus (pulvinar and dorso-median nuclei) (table 1 – see Additional file 1, fig. 1). Deactivated regions in the Target condition, were the superior frontal sulcus bilaterally, the left inferior frontal gyrus, the right posterior insula, the precuneus and the posterior cingulate bilaterally, the posterior part of the superior temporal sulcus, and infero-temporal areas (table 1 – see Additional file 1, fig. 1).

The Novel condition induced activation in the left inferior frontal sulcus and the occipital regions bilaterally extending to the left lateral temporal and posterior parietal areas (table 1 – see Additional file 1, fig. 1). The graphs in figure 1 represent the peristimulus BOLD signal for each condition in relevant regions after regressing the effect of the other conditions. The absence of Novel-related activation in the regions said to be the sources of the P300, as shown by peristimulus BOLD responses, allowed to ascertain that this observation, was neither due to a threshold effect nor to an inappropriate statistical analysis model.

EEG results

The N200 and P300 potentials were recorded for both Target and Novel conditions on the medial electrodes (Fz, Cz, Pz), with extension on both centrals (C3, C4). Significant differences in amplitude were found at the local, time-cluster and global levels, that were even greater in the Novel than in the Target condition for Cz, Pz, C3 and C4 (fig. 2). This was evidenced in all the subjects on electrode Cz, with a conjunction probability of $p = 0.000025$ (see table 1 for subject by subject results at 400 ms).

EROs also presented a statistical difference between the Target and Novel conditions, but in an opposite manner. Figure 2 shows the statistical comparison map between Targets (red) and Novels (blue). Targets evoked a greater increase in power than Novels between 200 and 500 ms in the 32-Hz band in F7, Cz, C3, C4 and Pz, and in the 34-Hz band in Fz and F8. Figure 3 (top) shows the time

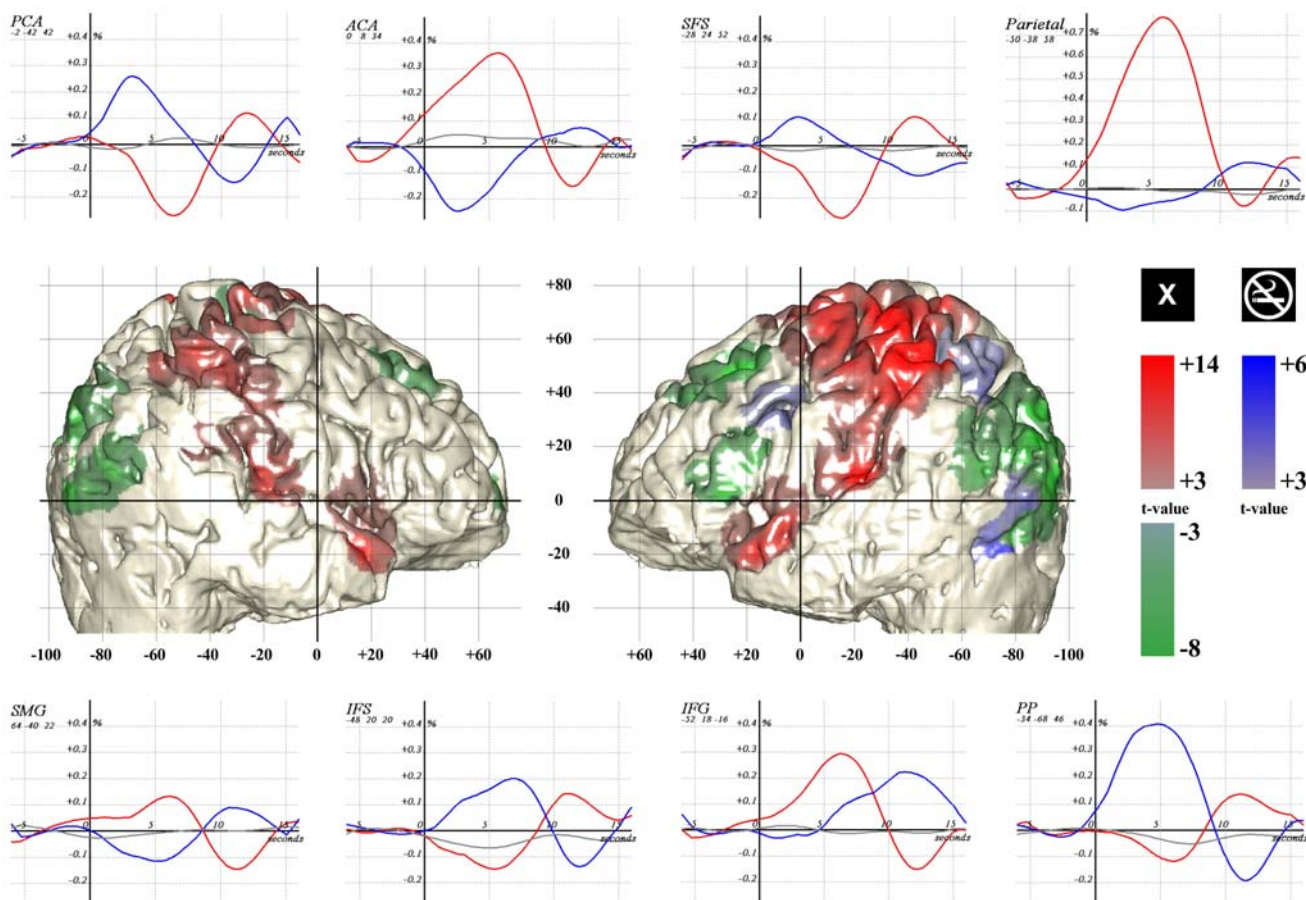


Figure 1
fMRI results Lateral views of the normalized brain of 1 subject, colored as a function of contrast: Target-related activation (red and "X" marks), Target-related deactivation (green and "no-smoking" marks), and Novel-related activation (blue) (thresholds $p \leq 0.001$, 100 voxel). The network that deactivated on target presentation comprised the superior frontal sulcus (SFS), the parietal cortex and the inferior frontal sulcus (IFS). The latter is supposed to be related with distractor inhibition since its posterior part is over-activated by Novels together with the posterior parietal cortex (PP). The network activated by targets comprised the supra-marginal gyrus (SMG) and the inferior frontal gyrus (IFG). Note that the TPJ is composed of the SMG (BA 40) in its upper part, and of the superior temporal gyrus (BA 39) in its lower part. The peristimulus BOLD signals are displayed for each relevant region for Targets (red), Novels (blue) and frequent distractors (gray). The curves are computed by simple averaging after regressing the other condition effect and removing high- and low-frequency components. The variation in signal intensity is indicated as a percentage of the MRI signal, and the scale is similar for all except the parietal area. Notice the balance between the anterior cingulate area (ACA) and the posterior cingulate area (PCA). Those charts also exclude the possibility for a threshold effect to account for the absence of Novel-related activation of the EXO network.

frequency chart for all the electrodes, for Targets (right) and Novels (left), with color-coded standard deviation relative to the reference distribution (-320 to 0 ms). There was a greater difference between the Target and Novel conditions in the 200 to 500 ms interval for the 32- to 38-Hz band. This was confirmed by the statistical map used to compare the two conditions (fig. 3 lower part), with two significant time-frequency clusters between 200 and 500 ms at 32 Hz ($p = 0.002$) and 38 Hz ($p = 0.001$) and a

global significance of $p < 0.0005$. There was no significant time-frequency point for the reverse statistics (Novels > Targets). Subject-by-subject conjunction analysis produced the same results, with a multi-subject conjunction probability of $p = 0.0014$ on electrode Cz at 38 Hz and 320 ms (see table 1 for subject by subject results). It could be argued that EROs were found to be larger in the Target condition, relative to the Novel condition, owing to the limited frequency range explored, so that we performed

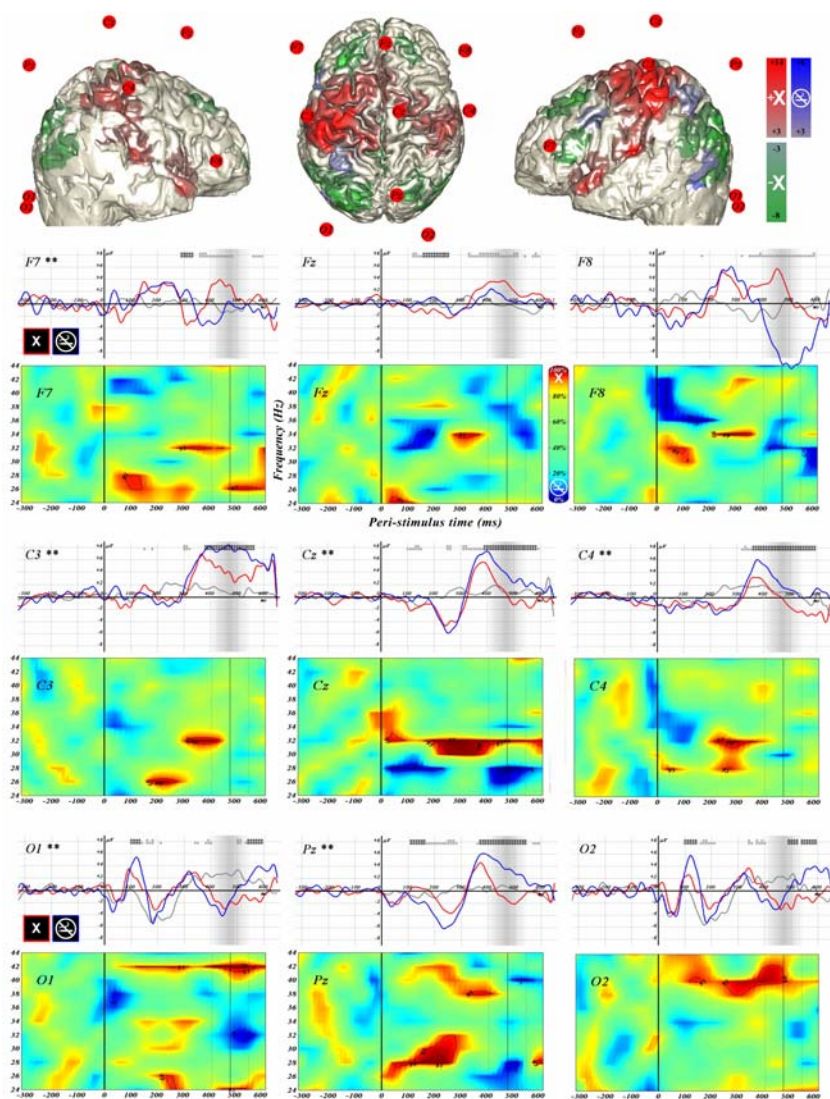


Figure 2

Evoked potentials and event-related oscillations for each electrode and for all the subjects. The upper part presents three different views of the average electrode position relative to the areas with BOLD activation (threshold $p \leq 0.001$, 100 voxels, Target-related activation – red, Target-related deactivation – green, and rare Distractor (Novel) activation – blue). It is provided for better appreciation of electrical signals, considering fMRI activation. The lower part displays the evoked potentials (EPs) and event-related oscillations (EROs) for each electrode, for the 5 subjects. For C3, Cz, C4, Pz, the "no-smoking" symbol, which is an instance of Novels (blue), yielded larger EPs than Targets (red). Distractors are represented in gray. For all the electrodes, the reverse is true as far as EROs are concerned, with significantly more oscillations around 300–400 ms, regarding Targets. In the case of EPs, signals have been plotted from -325 to +625 ms and the voltage range was kept constant from -9 to +9 μV . The shaded region around 474 ms corresponds to the response time and its standard deviation. The statistics for the comparison of Target-related and Novel-related EPs are computed every 10 ms, between 100 ms and 600 ms, and represented by the gray and black stars above the curves (1 star for $p_{nc} \leq 0.05$, 2 stars for $p_{nc} \leq 0.01$). The time-cluster significance, corrected for multiple comparison is indicated by the color of the stars: black if above $p_c \leq 0.05$, gray if not significant at the corrected time-cluster level. The set level is given for each electrode by the number of stars beside the electrode label (1 star for $p \leq 0.05$, 2 stars for $p \leq 0.01$). For EROs, only the statistics comparing Targets and Novels is given for the 24- to 44-Hz band, and between -320 to 600 ms. The solid and dotted black lines correspond to the response time and standard deviation, respectively. The color code for the statistics is shown on the upper right hand side, and represents the cumulative p distribution stated in percent. Cold colors code for a higher Novel-related power level, and hot colors code for greater Target-related power intensity. Regions above the .05 and .01 thresholds are contoured in black (notice that the numbers 1, 5, 95 and 99 represent the cumulative p values stated in percent).

Table 2: Subject by subject EPs and EROs results

Cz		P300 et 400 ms (μV)			EROs at 32 Hz and 320 ms (std)		
subjects	Targets	Novels	perm-test	Targets	Novels	perm-test	
1	15.6	15.8	0.08	9.7	2.1	0.01	
2	1.1	4.6	0.01	12.2	4.8	0.04	
3	3.0	7.6	< 0.01	10.4	5.8	0.08	
4	2.0	2.9	0.12	5.0	4.2	0.27	
5	6.5	7.6	0.08	9.7	6.5	0.25	
Mean	5.6	7.7		9.4	4.7		
Std	5.9	5.0		2.7	1.7		

Both are given for the Cz electrode, the P300 is given in micro-Volts (μV), 400 ms after stimulus presentation, (highest statistical difference in the group analysis), and EROs are given in standard deviation relative to the pre-stimulus period, at 38 Hz, 320 ms after stimulus presentation (highest value in the group analysis). The results of the permutation test were obtained for each subject as explained in the method section.

further analysis in the 25- to 200-Hz range, every 5 Hz. Between 100 and 400 ms, and considering an uncorrected $p \leq 0.01$ for report, Novels failed to present larger EROs than Targets, whereas the latter presented larger EROs at 35, 95, 110 and 140 Hz (additional material available on request).

Discussion

After confronting these results with those of prior reports, we propound physiological hypotheses to account for this discrepancy between EPs and fMRI/EROs.

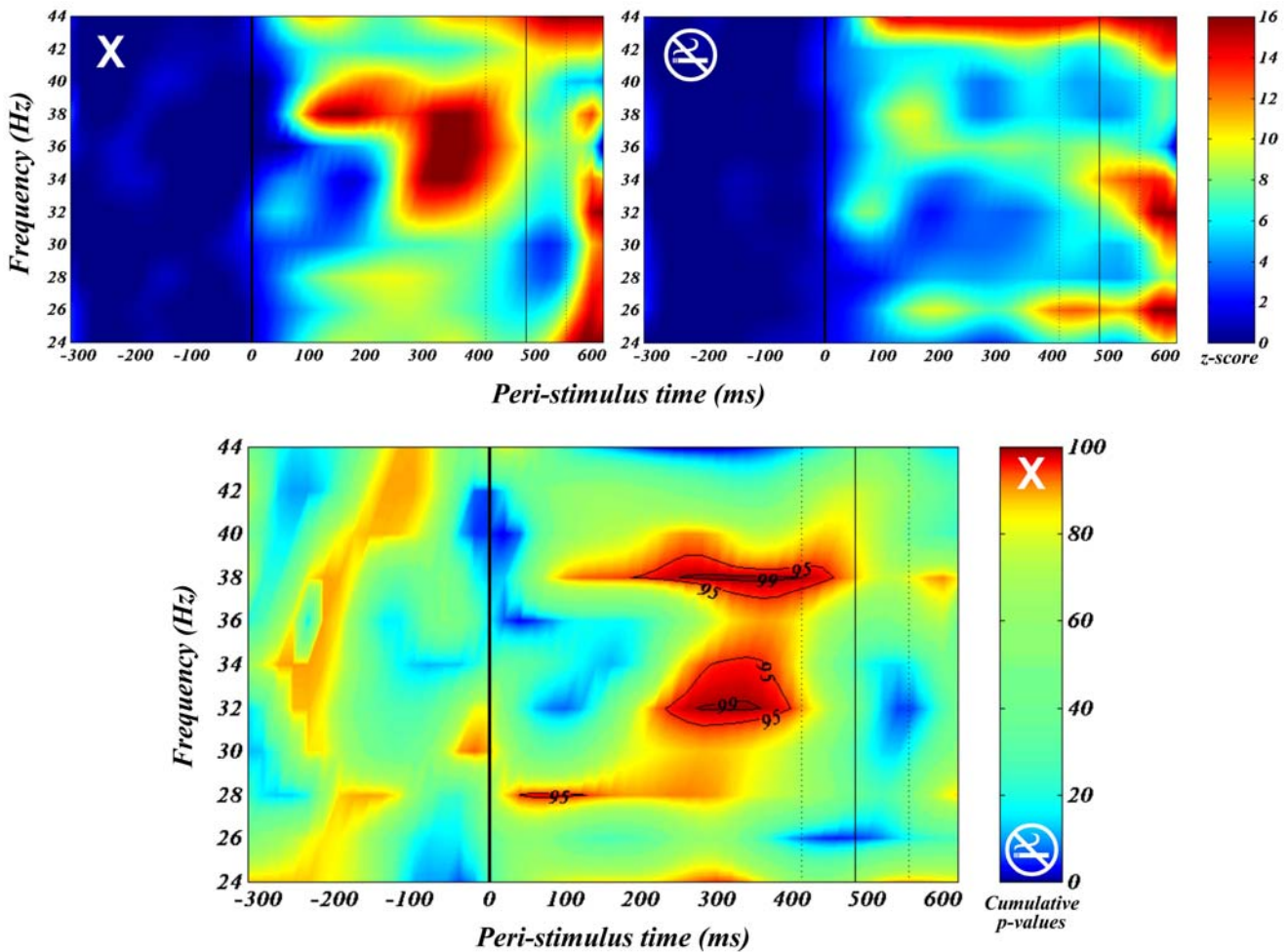
In accordance with previous experiments, Novels yielded a P300 of significantly greater amplitude than Targets [6]. The relatively low amplitude of the P300, about 8 μV , compared to the expected 10 to 20 μV [6], might well be related to the use of a common reference [26]. However, we cannot rule out the possibility that part of the P300 could have been regressed with the electro-cardio-balistic artifact in some trials. The principal component of the pulse artifact looks like a damped oscillation around 7.5 Hz [27] (Otzenberger et al. submitted) which includes part of the theta component of the P300 [6,28]. However discarding trials in which the largest part of the pulse artifact covered the 300 to 400-ms post-stimulus period in two subjects did not modify their results. Even so, the pulse artifact should equally affect Target- and Novel-related P300 without affecting the difference between them.

Our fMRI results are also in line with the literature [13,14,16,29–36]. The putative sources of the P300, the temporal-parietal junction and the inferior frontal gyrus [8], were only activated in the Target condition by all the subjects. Novels activated the left inferior frontal sulcus that was part of a network deactivated by Targets. This region might well support response inhibition [37–44].

Our EROs results not only nicely reproduce results reported in previous studies, regarding the frequency (38 Hz) and the delay (360 ms) [22–25], but go one step further by showing that over a large frequency range, and between 100 and 400 ms, Targets triggered larger EROs than Novels. Accordingly, the differential reactivity of Target- and Novel-related EROs was in line with that of fMRI. An important limitation of this study however, is that, owing to the limited number of electrodes, we were unable to ascertain whether EROs arose from the same sources as EPs. Yet, the differential effect seems to take place on the same electrodes, as if the dipoles had the same scalp projection. Subsequent intra-cranial or inverse solution experiments are required to establish this point.

From a cognitive point of view, this discrepancy between EPs on one hand and EROs and fMRI on the other hand, may originate from several, possibly interacting, processes: i) different processing for Targets and Novels, related with differences in attentional requirement, ii) different visual processing for the letter "X" and pictures, iii) a different susceptibility to stimulus repetition. Further studies are required to clarify this point, but the interesting fact is that EPs react in an opposite way to fMRI, whereas EROs responds in the same way.

Such discrepancy between EPs and the fMRI signal may not be unique. There is at least one other condition where EPs and fMRI may not present the same differential reactivity. In episodic memory, the contrast between correct recognition of old items vs. correct rejection of distractors activates the left frontal lobe in fMRI [45–47]. On the other hand, performing a source analysis based on EPs from EEG and magneto-encephalographic (MEG) data fails to evidence activity in this region [21]. Interestingly enough, in this last study, the time frequency analysis showed a difference in the gamma range projecting on the



Volume Level	Cluster Level		Voxel Level		TF coordinates	
	p(cor)	equivk	p(cor)	p(nc)	Frq (Hz)	Time (ms)
< 0.0005	0.001	160	0.17	0.0015	38	320
	0.002	80	0.33	0.0050	32	320

Figure 3

Event-related oscillations for all the electrodes. The upper part presents the event-related oscillations (EROs) time-frequency chart for Targets on the left (X-mark), and rare distractors (Novels) on the right ("no-smoking" symbol). It is shown for the 24- to 44-Hz band, and between -320 to 600 ms, summing up all 9 electrodes for all the subjects. The color scale represents the relative amount of power in standard deviation (reference period from -320 to 0 ms). This illustrates that the 32- to 38-Hz EROs in response to Targets are quite low in response to Novels. It thus does not come as a surprise that the statistical comparison of Target-related vs. Novel-related power for all electrodes is significant (lower time-frequency chart). Cold colors code for a trend towards greater power in the Novel condition, whereas hot colors represent greater power level in the Target condition. The scale represents the cumulative p distribution stated in percent. Regions above the .05 and .01 threshold are contoured in black. The numbers 1, 5, 95 and 99 represent the cumulative p value in percent, respectively equivalent to .01, .05 for Novels and .05, .01 for Targets. The solid and dotted black lines correspond to the response time and standard deviation, respectively. The result table provides the statistics for the time interval from 200 to 500 ms, and from 24 to 44 Hz, using a threshold $p \leq 0.01$. Volume and time-frequency cluster p values are given corrected for multiple comparisons. Note that the ensemble statistics represent the probability to have the given amount of time-frequency points above the threshold (12 over 165 time-frequency points), and not the number of clusters as in EPs or fMRI. At the same threshold, there were no significantly larger power emissions in the Novel than in the Target condition (not even at the .05 threshold).

left fronto-temporal electrodes / MEG sensor position [21].

Our study provides direct evidence that gamma oscillations better match the BOLD signal than EPs do. This observation is well in line with other works on animals. Logothetis and co-workers successfully recorded the BOLD response together with the equivalent of local field potentials in the visual cortex of anesthetized monkeys. They observed that the best correlation was achieved when taking frequencies in the gamma range [5,48].

The reason why EROs seem to correlate better with the BOLD signal than EPs do, remains, as yet, uncertain. The EEG and BOLD signals both reflect synaptic activity [2–5,49,50]. But EEG and fMRI integrate synaptic activity over different time windows [2–5]. The former reflects synchronous firing of synapses within milliseconds [49,50]. On the other hand, fMRI represents the integration of synaptic activity over several hundreds of milliseconds [1]. Thus a small jitter of the neuronal response relative to a stimulus e.g. tens of milliseconds, will dramatically affect the averaging of EPs [20] but will only have a limited impact on the averaging of BOLD responses. On the other hand, EROs do not require to be time-locked to the stimulus so precisely, and will average well despite such jitter [20]. Taking this jitter into account might even become crucial as one considers higher cognitive tasks. With the involvement of decisions requiring longer response times, uncertainty about the time of involvement of some areas might well increase [21]. This however only provides partial explanation, as there is no reason to believe that the jitter affecting Target-related P300 should exceed that affecting Novel-related P300.

A second reason could be related to the fact that EEG and BOLD signals reflect the activity of different cell populations. EEG reflects the synaptic input function of pyramidal cells only, i.e. post-synaptic potential, either excitatory or inhibitory [49,50], whereas fMRI reflects the synaptic activity of all neural cells [2–5]. There is no particular reason for EPs to rely on anything else than pyramidal cell synaptic activity, but it has been demonstrated that synchronous oscillations require the involvement of inhibitory interneurons together with pyramidal cells [51,52]. Accordingly, EPs and EROs might reflect different kinds of neuronal activity, and the BOLD signal might be more sensitive to EROs because of the larger amount of contributing cells and synapses. Animal works illustrate how those two kinds of activity emerge in a task similar to the one we used. If a behaving monkey is presented with an object, but attends to another (analogous to the Novel condition), one only observes a phasic rise in spiking activity lasting for about 50 ms that could well go with an EP on the scalp [53,54]. But if the object attended to is

presented (analogous to the Target condition), the phasic rise is followed by gamma oscillations for 300 ms [55,56].

Last, it must be noted that positive correlation with the BOLD signal seems only to apply to fast oscillations (> 15-Hz), whereas slow waves, below 12 Hz, were reported to be negatively correlated with the fMRI signal [57] (Foucher et al. submitted). This should not be surprising as low and high frequencies have been described to correlate negatively [58]. The discrepancy observed between EROs and EPs, might be considered not so much as a matter of whether activity is phase-locked or not, but rather as a matter of frequency. Should this be the case, the P300, which ranges in the theta frequency spectrum (4-8Hz) [6], may not be well suited to be positively correlated with BOLD. Unfortunately our methodology did not allow us to test whether or not theta EROs differed from the P300 reactivity (the 7-cycle wavelet would not have fitted in the EEG window limited by gradient artifacts). However, it has been shown in different protocols, that EP frequencies are not necessarily enhanced on the EROs analysis [59]. This calls into question the kind of neuronal activity responsible for the generation of an evoked potential. It has been suggested that part of an EP could correspond to the simple phase resetting of ongoing cerebral activity [59,60]. Should this turn out to be true, since phase resetting should not consume much energy, it could be another reason why EPs and BOLD signals are not well correlated.

Conclusion

This is the first direct demonstration of an inverse differential reactivity between EPs and the BOLD signal arising from the same brain activity. This observation has to be taken into account for the integration of the EEG and the fMRI data. In the light of this attempt, these results plead for taking into account the EEG oscillatory response, as it was shown to share the same differential reactivity as the BOLD signal. Further explorations are called for to work out the reasons underlying this phenomenon, but it can be suggested that this is because the BOLD signal and EROs are less sensitive to random jitter of the brain response, and because they rely on neural activity of another kind than EPs, involving different population of cells. Differential reactivity is an interesting paradigm to explore the relationship between the BOLD and EEG signals, since the level of noise makes direct correlation between EPs, EROs and BOLD difficult. Further studies, involving different tasks and stimuli, should also consider the localization of the electrical activity using a larger amount of electrodes.

Methods

Subjects and task

Five subjects with no prior history of neurological injury (4 right-handed, 1 left-handed, 3 females, aged 18 to 23 years) gave informed consent prior to participating in this study approved by the local ethical committee. Visual stimuli were presented to them, consisting in series of Frequent Distractors (repeating the same letter "O", 47%), Novels (7%, black and white namable pictures, never repeated), and rare Targets (always the same letter "X", 7%). The proportion of white pixels was kept in the same range for all stimuli to avoid stimulus intensity changes ($\sim 20\%$). Although pictures were kept as simple as possible (pictograms such as a heart, flash of lightning) some were more complex than the letters (e.g. no-smoking, danger or nuclear signs). All the stimuli were square pictures covering $\sim 5^\circ$ of the visual field, which were presented for 70 ms using the software *expe6* [61]. The subjects were instructed to signal Targets by pressing a response key with the right forefinger, and to ignore other stimuli. The remaining 39% were null events (empty screen). All the stimuli were presented pseudo-randomly to maximize the contrasts [62]. Inter-stimuli intervals were homogeneously distributed from 0.4 to 3.6 s (median of 2 s) and intervals between two Targets ranged from 5.2 to 96 s [63]. Each subject performed two sessions involving this 3-stimulus paradigm.

fMRI acquisition

In order to record gradient artifact-free EEG data simultaneously with fMRI, the volumes were separated by a 1,6-s period during which gradients were not commuted [17,18]. Single-shot gradient echo, echo planar imaging was used for the functional study, relying on the BOLD effect (Bruker 2T / 270 volumes preceded by 5 dummy scans for steady state of T_1 partial saturation effect / $TR = 4$ s / Imaging time = 2.6 s / flip angle of 90° / $TE = 43$ ms / 4-mm in-plane resolution, FOV = 256 mm, gridding 64^2 , 4-mm slice thickness / 24 slices covering the whole brain except for the cerebellum). Thirty-five rare stimuli out of 40 were presented during the no-gradient period for each condition. This asymmetry escaped all participants' notice. A RARE sequence was used for the acquisition of anatomical images including electrode positioning, thanks to accompanying MRI markers ($2T / TR = 15$ s / $TE = 73.8$ ms / 2-mm in-plane resolution, FOV = 256 mm, gridding 128^2 , 2-mm slice thickness / 60 slices).

fMRI processing

The volumes were realigned, normalized (voxel size after re-sampling : 2 mm isotropic) and smoothed with an 8-mm kernel under SPM99 [64]. The data were further processed through pass-band filtering (the hemodynamic response for low-pass filter, and 47-s cut-off for high-pass filter) and the voxel intensity was scaled relative to the

global volume. For the purpose of the statistical analysis, the brain responses to Targets, Novels and Distractors were modeled as stick functions convolved with a hemodynamic response and its temporal derivative. The analysis was looking for regions significantly correlated with those functions in the context of the general linear model [65]. The statistics are provided in two ways: i) a fixed effect, one-tail t-test, to enable comparison between fMRI and EEG results ($p \leq 0.001$ uncorrected, cluster size > 100 voxels = 800 mm^3), and ii) multi-subject conjunction analysis to allow the extrapolation of the results obtained to the population [66,67]. The results are given using a threshold $p \leq 0.05$ uncorrected for each individual t-map, which is equivalent to a conjunction probability of $p \leq 3.1 \cdot 10^{-7}$ (uncorrected). For all maximally activated voxel per cluster, the minimal percentage of the population that should display activity at $p \leq 0.05$ is given uncorrected, using a 95% confidence interval, and assuming the test sensitivity to be 100% (formula $n^{\circ 3}$ in [67]).

EEG acquisition

The EEG was recorded using 10 shielded electrodes at the F7-Fz-F8-C3-Cz-C7-Pz-O1-O2-A2 sites according to the international 10/20 standard [68], with ground on the nasion. Data were recorded with a referential montage to a common reference, using an MRI-compatible device (Schwarzer – GE). Conductances were tested out of the magnet and remained below 5 kOhm, except for C3 in 2 sessions (data excluded from the analysis). The ECG was amplified separately (Bruker – GE). Signals were sampled at 1000 Hz with pre-amplification filters set from 0.003 to 300 Hz.

EEG processing

The electro-cardio-balisto-graphic artifact [69] (or pulse artifact) was removed by regression of the first eigenvector computed from a set of pulse artifacts taken as a reference at the beginning of the experiment (~ 80 of 700 ms each, the first eigenvector accounted for more than 30 % of the variance). The signal was further band filtered from 0.1 to 20 Hz using a Fourier-based method [70], and EPs were computed by averaging the signals between -325 and +625 ms, after having discarded the trials whose amplitude variation exceeded $100 \mu\text{V}$ (there remained 26 ± 4 trials out of 35, per condition and per session) [63]. EROs were computed from the same data set without prior filtering. For each trial and electrode, the signal was first filtered in the ± 2 -Hz band every 2 Hz between 24 and 44 Hz, then convoluted with a complex 7-cycle Morlet wavelet [71–73]. The module of the convolution product represents the power integrated over a window equivalent to 7 cycles, thus adapted to each frequency [71,73]. The result was normalized for each frequency using the first 320-ms period before stimulus presentation, and down-sampled to 50 Hz (20-ms period).

The statistical comparison of Target- and Novel-related EPs and EROs was carried out using a randomization approach [74]. First, the effective difference between Targets and Novels was computed. Next, Target and Novel trials were put together and randomized, subsequently separated into two groups from which a new difference was computed. By repeating this procedure 2000 times, a reference distribution of the differences was established every 10 ms for EPs and every 50 ms for EROs. The effective difference was compared to this distribution for each electrode and each time point, using a threshold of 0.05 and 0.01 (one-tail). In order to take into account multiple comparisons, the probability to obtain a given time-cluster size and the total amount of significant points (ensemble level) was assessed from the same randomized set between 200 and 500 ms for each electrode (in the 24- to 44-Hz band for EROs) and using a threshold of 0.01 for report (one-tail). The same statistics were also used to perform subject-by-subject conjunction analysis on electrode Cz to verify that the results thus obtained were not due to a few subjects out of the five, and to allow extrapolation to the population.

List of abbreviations

fMRI Functional Magnetic Resonance

BOLD Blood Oxygen Level Dependent

EEG Electro-Encephalography

ECG Electro-Cardiograph

MEG Magneto-Encephalography

ERO Event Related Oscillations

EP Evoked Potentials

Authors' contributions

JF contributed to the conception, design and analysis of the study, and drafted the manuscript. HO contributed to setting up EEG-fMRI recording and to the analysis of evoked potentials data. DG contributed to the design, EEG-fMRI settings, and fMRI analysis. All authors have read and approved the final manuscript.

Additional material

Additional File 1

Description of the clusters activated (Targets+) or deactivated (Targets-) by the Targets, and activated by rare distractors (Novels+), together with their respective projection on a transparent brain. The fixed effect statistical values are given for a threshold $t = 3.10$ ($p_{nc} = 0.001$ one-tail, $df = 1593.7$) with an extent threshold of 100 voxels ($p_{nc} = 0.004$, $p_c = 0.059$ corrected, 1 resel = 106 voxels). The first column presents the probability to obtain the specified number of clusters (second column). The third column indicates the corrected probability for each cluster, and the fourth column, the number of voxels per cluster. The fifth column presents the corrected probability for the given voxel together with the uncorrected Target and p values (sixth and seventh column). For the same voxel, the eighth column provides the results of the subject conjunction analysis for "population inference" in two ways. If the voxel is active in all the subjects at $p_{nc} \leq 0.05$, then the minimal percentage of the population that should present at least the same significance level is given (95% confidence interval). If one or more subjects are below that threshold, then the lowest significance is given in p value. The MNI coordinates together with the anatomical sites and Brodmann areas are provided in the subsequent columns. Smoothness: FWHM = $9.6 \times 9.6 \times 9.3$ mm. Search volume: 1337 cm³ (167142, $2 \times 2 \times 2$ -mm voxels).

Click here for file

[<http://www.biomedcentral.com/content/supplementary/1471-2202-4-22-S1.pdf>]

Acknowledgments

We are thankful to Dr Jean-Philippe Lachaux, Dr Jean-Baptiste Poline, Pr Daniel Grucker, and Pr Jean-Marie Danion for reading the manuscript and fruitful criticism, as well as to the whole Dynamic Neuronal Activity group of the LENA for their contribution to data analysis. A special thanks to Pr John Polich who provided critical advice, especially about how to adapt our treatment of EP data and about their interpretation. We would also like to thank Mrs Corinne Marrer for her hard-working contribution in the acquisition of fMRI data, Mrs Monique Noël and the whole neurological ward for skillful electrode placement. We are grateful to Pr Guy Foucher, and Ms Nathalie Heider for correcting our manuscript. The UMR 7004 ULP/CNRS – Strasbourg, supported this work.

References

1. Aine CJ: **A conceptual overview and critique of functional neuroimaging techniques in humans: I. MRI/fMRI and PET.** *Crit Rev Neurobiol* 1995, **9**:229-309.
2. Mathiesen C, Caesar K, Akgoren N and Lauritzen M: **Modification of activity-dependent increases of cerebral blood flow by excitatory synaptic activity and spikes in rat cerebellar cortex.** *J Physiol* 1998, **512**:555-566.
3. Mathiesen C, Caesar K and Lauritzen M: **Temporal coupling between neuronal activity and blood flow in rat cerebellar cortex as indicated by field potential analysis.** *J Physiol* 2000, **523(Pt 1)**:235-246.
4. Matsuura T and Kanno I: **Quantitative and temporal relationship between local cerebral blood flow and neuronal activation induced by somatosensory stimulation in rats.** *Neurosci Res* 2001, **40**:281-290.
5. Logothetis NK, Pauls J, Augath M, Trinath T and Oeltermann A: **Neurophysiological investigation of the basis of the fMRI signal.** *Nature* 2001, **412**:150-157.
6. Polich J: **Neuropsychology of P3a and P3b: a theoretical overview.** In *Advances in electrophysiology in clinical practice and research* Edited by: Arikan K, Moore N. Wheaton: Kjellberg; 2002.
7. Lopes da Silva FH: **Event-related potentials: Methodology and quantification.** In *Electroencephalography, basic principles, clinical applications and related fields* Edited by: Niedermeyer E, Lopes da Silva F. Williams & Wilkins; 1999:947-957.
8. Soltani M and Knight RT: **Neural origins of the P300.** *Crit Rev Neurobiol* 2000, **14**:199-224.

9. Halgren E, Baudena P, Clarke JM, Heit G, Liegeois C and Chauvel P et al.: **Intracerebral potentials to rare target and distractor auditory and visual stimuli. I. Superior temporal plane and parietal lobe.** *Electroencephalogr Clin Neurophysiol* 1995, **94**:191-220.
10. Halgren E, Baudena P, Clarke JM, Heit G, Marinkovic K and Devaux B et al.: **Intracerebral potentials to rare target and distractor auditory and visual stimuli. II. Medial, lateral and posterior temporal lobe.** *Electroencephalogr Clin Neurophysiol* 1995, **94**:229-250.
11. Courchesne E, Hillyard SA and Galambos R: **Stimulus novelty, task relevance and the visual evoked potential in man.** *Electroencephalogr Clin Neurophysiol* 1975, **39**:131-143.
12. Knight RT: **Decreased response to novel stimuli after prefrontal lesions in man.** *Electroencephalogr Clin Neurophysiol* 1984, **59**:9-20.
13. Clark VP, Fannon S, Lai S and Benson R: **Paradigm-dependent modulation of event-related fMRI activity evoked by the oddball task.** *Hum Brain Mapp* 2001, **14**:116-127.
14. Clark VP, Fannon S, Lai S, Benson R and Bauer L: **Responses to rare visual target and distractor stimuli using event-related fMRI.** *J Neurophysiol* 2000, **83**:3133-3139.
15. Kirino E, Belger A, Goldman-Rakic P and McCarthy G: **Prefrontal activation evoked by infrequent target and novel stimuli in a visual target detection task: an event-related functional magnetic resonance imaging study.** *J Neurosci* 2000, **20**:6612-6618.
16. Kiehl KA and Liddle PF: **An event-related functional magnetic resonance imaging study of an auditory oddball task in schizophrenia.** *Schizophr Res* 2001, **48**:159-171.
17. Bonmassar G, Anami K, Ives J and Belliveau JW: **Visual evoked potential (VEP) measured by simultaneous 64-channel EEG and 3T fMRI.** *Neuroreport* 1999, **10**:1893-1897.
18. Kruggel F, Wiggins CJ, Herrmann CS and von Cramon DY: **Recording of the event-related potentials during functional MRI at 3.0 Tesla field strength.** *Magn Reson Med* 2000, **44**:277-282.
19. Varela FJ, Lachaux JP, Rodriguez E and Martinerie J: **The brainweb : phase synchronization and large-scale integration.** *Nature Reviews in Neuroscience* 2001, **2**:229-239.
20. Tallon-Baudry C and Bertrand O: **Oscillatory gamma activity in humans and its role in object representation.** *Trends Cogn Sci* 1999, **3**:151-162.
21. Duzel E, Habib R, Schott B, Schoenfeld A, Lobaugh N and McIntosh AR et al.: **A multivariate, spatiotemporal analysis of electro-magnetic time-frequency data of recognition memory.** *Neuroimage* 2003, **18**:185-197.
22. Marshall L, Molle M and Bartsch P: **Event-related gamma band activity during passive and active oddball tasks.** *Neuroreport* 1996, **7**:1517-1520.
23. Fell J, Hinrichs H and Roschke J: **Time course of human 40 Hz EEG activity accompanying P3 responses in an auditory oddball paradigm.** *Neurosci Lett* 1997, **235**:121-124.
24. Haig AR, De PV and Gordon E: **Peak gamma latency correlated with reaction time in a conventional oddball paradigm.** *Clin Neurophysiol* 1999, **110**:158-165.
25. Gurtubay IG, Alegre M, Labarga A, Malanda A, Iriarte J and Artieda J: **Gamma band activity in an auditory oddball paradigm studied with the wavelet transform.** *Clin Neurophysiol* 2001, **112**:1219-1228.
26. Reilly EL: **EEG recording and operation of the apparatus.** In *Electroencephalography, basic principles, clinical applications and related fields* Edited by: Niedermeyer E, Lopes da Silva F. Williams & Wilkins; 1999:122-142.
27. Schomer DL, Bonmassar G, Lazeyras F, Seeck M, Blum A and Anami K et al.: **EEG-Linked functional magnetic resonance imaging in epilepsy and cognitive neurophysiology.** *J Clin Neurophysiol* 2000, **17**:43-58.
28. Demiralp T, Ademoglu A, Comerchero M and Polich J: **Wavelet analysis of P3a and P3b.** *Brain Topogr* 2001, **13**:251-267.
29. Menon V, Ford JM, Lim KO, Glover GH and Pfefferbaum A: **Combined event-related fMRI and EEG evidence for temporal-parietal cortex activation during target detection.** *Neuroreport* 1997, **8**:3029-3037.
30. McCarthy G, Luby M, Gore J and Goldman-Rakic P: **Infrequent events transiently activate human prefrontal and parietal cortex as measured by functional MRI.** *J Neurophysiol* 1997, **77**:1630-1634.
31. Yoshiura T, Zhong J, Shibata DK, Kwok WE, Shrier DA and Numaguchi Y: **Functional MRI study of auditory and visual oddball tasks.** *Neuroreport* 1999, **10**:1683-1688.
32. Stevens AA, Skudlarski P, Gatenby JC and Gore JC: **Event-related fMRI of auditory and visual oddball tasks.** *Magn Reson Imaging* 2000, **18**:495-502.
33. Downar J, Crawley AP, Mikulis DJ and Davis KD: **A cortical network sensitive to stimulus salience in a neutral behavioral context across multiple sensory modalities.** *J Neurophysiol* 2002, **87**:615-620.
34. Downar J, Crawley AP, Mikulis DJ and Davis KD: **A multimodal cortical network for the detection of changes in the sensory environment.** *Nat Neurosci* 2000, **3**:277-283.
35. Downar J, Crawley AP, Mikulis DJ and Davis KD: **The effect of task relevance on the cortical response to changes in visual and auditory stimuli: an event-related fMRI study.** *Neuroimage* 2001, **14**:1256-1267.
36. Corbetta M and Shulman GL: **Control of goal-directed and stimulus-driven attention in the brain.** *Nat Rev Neurosci* 2002, **3**:201-215.
37. Liddle PF, Kiehl KA and Smith AM: **Event-related fMRI study of response inhibition.** *Hum Brain Mapp* 2001, **12**:100-109.
38. Konishi S, Nakajima K, Uchida I, Kikyo H, Kameyama M and Miyashita Y: **Common inhibitory mechanism in human inferior prefrontal cortex revealed by event-related functional MRI.** *Brain* 1999, **122**(Pt 5):981-991.
39. Konishi S, Nakajima K, Uchida I, Sekihara K and Miyashita Y: **No-go dominant brain activity in human inferior prefrontal cortex revealed by functional magnetic resonance imaging.** *Eur J Neurosci* 1998, **10**:1209-1213.
40. Fallgatter AJ, Brandeis D and Strik WK: **A robust assessment of the NoGo-antiorisation of P300 microstates in a cued Continuous Performance Test.** *Brain Topogr* 1997, **9**:295-302.
41. Sasaki K, Gemba H, Nambu A and Matsuzaki R: **No-go activity in the frontal association cortex of human subjects.** *Neurosci Res* 1993, **18**:249-252.
42. Fallgatter AJ, Esienack SS, Neuhauser B, Aranda D, Scheuerpflug P and Herrmann MJ: **Stability of late event-related potentials: topographical descriptors of motor control compared with the P300 amplitude.** *Brain Topogr* 2000, **12**:255-261.
43. Bisiach E, Mini M, Sterzi R and Vallar G: **Hemispheric lateralization of the decisional stage in choice reaction times to visual unstructured stimuli.** *Cortex* 1982, **18**:191-197.
44. Vallar G, Bisiach E, Cerizza M and Rusconi ML: **The role of the left hemisphere in decision-making.** *Cortex* 1988, **24**:399-410.
45. Konishi S, Wheeler ME, Donaldson DI and Buckner RL: **Neural correlates of episodic retrieval success.** *Neuroimage* 2000, **12**:276-286.
46. McDermott KB, Jones TC, Petersen SE, Lageman SK and Roediger HL III: **Retrieval success is accompanied by enhanced activation in anterior prefrontal cortex during recognition memory: an event-related fMRI study.** *J Cogn Neurosci* 2000, **12**:965-976.
47. Donaldson DI, Petersen SE, Ollinger JM and Buckner RL: **Dissociating state and item components of recognition memory using fMRI.** *Neuroimage* 2001, **13**:129-142.
48. Logothetis NK: **The neural basis of the blood-oxygen-level-dependent functional magnetic resonance imaging signal.** *Philos Trans R Soc Lond B Biol Sci* 2002, **357**:1003-1037.
49. Speckmann EJ and Elger CE: **Introduction to the neurophysiological basis of the EEG and DC potentials.** In *Electroencephalography, basic principles, clinical applications and related fields* Edited by: Niedermeyer E, Lopes da Silva F. Williams & Wilkins; 1999:15-27.
50. Baillet S, Mosher JC and Leahy RM: **Electromagnetic brain mapping.** *IEEE Signal Proc Mag* 2001, **18**:14-30.
51. Traub RD, Whittington MA, Colling SB, Buzsaki G and Jefferys JG: **Analysis of gamma rhythms in the rat hippocampus in vitro and in vivo.** *J Physiol* 1996, **493**(Pt 2):471-484.
52. Traub RD, Jefferys JG and Whittington MA: *Fast oscillations in cortical circuits* Cambridge MA: MIT Press; 1999.
53. Chelazzi L, Duncan J, Miller EK and Desimone R: **Responses of neurons in inferior temporal cortex during memory-guided visual search.** *J Neurophysiol* 1998, **80**:2918-2940.
54. Jagadeesh B, Chelazzi L, Mishkin M and Desimone R: **Learning increases stimulus salience in anterior inferior temporal cortex of the macaque.** *J Neurophysiol* 2001, **86**:290-303.

55. Engel AK, Fries P and Singer W: **Dynamic predictions: oscillations and synchrony in top-down processing.** *Nat Rev Neurosci* 2001, **2**:704-716.
56. Fries P, Reynolds JH, Rorie AE and Desimone R: **Modulation of oscillatory neuronal synchronization by selective visual attention.** *Science* 2001, **291**:1560-1563.
57. Goldman RI, Stern JM, Engel J Jr and Cohen MS: **Simultaneous EEG and fMRI of the alpha rhythm.** *Neuroreport* 2002, **13**:2487-2492.
58. Pfurtscheller G and Lopes da Silva FH: **Event-related EEG/MEG synchronization and desynchronization: basic principles.** *Clin Neurophysiol* 1999, **110**:1842-1857.
59. Tass PA: *Phase resetting in medicine an biology* Springer-Verlag; 1999.
60. Makeig S, Westerfield M, Jung TP, Enghoff S, Townsend J and Courchesne E et al.: **Dynamic brain sources of visual evoked responses.** *Science* 2002, **295**:690-694.
61. Pallier C, Dupoux E and Jeannin X: **Expe: an expandable programming language for on-line psychological experiments.** *Behavior Research Methods, Instruments and Computers* 1997, **29**:322-327.
62. Friston KJ, Zarahn E, Josephs O, Henson RN and Dale AM: **Stochastic designs in event-related fMRI.** *Neuroimage* 1999, **10**:607-619.
63. Polich J: **P300 in clinical applications.** In *Electroencephalography : basic principles, clinical applications and related fields* Edited by: Niedermeyer E, Lopes da Silva F. Baltimore: Williams & Wilkins; 1999:1073-1091.
64. Friston KJ, Holmes AP, Worsley KJ, Poline JB and Frackowiak RSJ: **Statistical parametric maps in functional imaging: a general linear approach.** *Hum Brain Mapp* 1995, **2**:189-210.
65. Josephs O and Henson RN: **Event-related functional magnetic resonance imaging: modelling, inference and optimization.** *Philos Trans R Soc Lond B Biol Sci* 1999, **354**:1215-1228.
66. Friston KJ, Holmes AP and Worsley KJ: **How many subjects constitute a study?** *Neuroimage* 1999, **10**:1-5.
67. Friston KJ, Holmes AP, Price CJ, Buchel C and Worsley KJ: **Multisubject fMRI studies and conjunction analyses.** *Neuroimage* 1999, **10**:385-396.
68. xx x: **American Electroencephalographic Society guidelines for standard electrode position nomenclature.** *J Clin Neurophysiol* 1991, **8**:200-202.
69. Allen PJ, Polizzi G, Krakow K, Fish DR and Lemieux L: **Identification of EEG events in the MR scanner: the problem of pulse artifact and a method for its subtraction.** *Neuroimage* 1998, **8**:229-239.
70. Hoffmann A, Jager L, Werhahn KJ, Jaschke M, Noachtar S and Reiser M: **Electroencephalography during functional echo-planar imaging: detection of epileptic spikes using post-processing methods.** *Magn Reson Med* 2000, **44**:791-798.
71. Lachaux JP, Rodriguez E, Martinerie J and Varela FJ: **Measuring phase synchrony in brain signals.** *Hum Brain Mapp* 1999, **8**:194-208.
72. Rodriguez E, George N, Lachaux JP, Martinerie J, Renault B and Varela FJ: **Perception's shadow: long-distance synchronization of human brain activity.** *Nature* 1999, **397**:430-433.
73. Le Van QM, Foucher J, Lachaux J, Rodriguez E, Lutz A and Martinerie J et al.: **Comparison of Hilbert transform and wavelet methods for the analysis of neuronal synchrony.** *J Neurosci Methods* 2001, **111**:83-98.
74. Nichols TE and Holmes AP: **Nonparametric permutation tests for functional neuroimaging: a primer with examples.** *Hum Brain Mapp* 2002, **15**:1-25.

Publish with **BioMed Central** and every scientist can read your work free of charge

"BioMed Central will be the most significant development for disseminating the results of biomedical research in our lifetime."

Sir Paul Nurse, Cancer Research UK

Your research papers will be:

- available free of charge to the entire biomedical community
- peer reviewed and published immediately upon acceptance
- cited in PubMed and archived on PubMed Central
- yours — you keep the copyright

Submit your manuscript here:
http://www.biomedcentral.com/info/publishing_adv.asp

